Supporting Information

Connell et al. 10.1073/pnas.1421211111

SI Text

Materials. FcMeOH (97%; 335061), Gelatin type A (G2500), and Rose Bengal (330000) were purchased from Sigma Aldrich. Lab-Tek four-well chambered coverglass (#1 borosilicate; 12–565-401) was supplied by Fisher Scientific. Glutaraldehyde (18426) was obtained from Ted Pella, Inc. A BacLight Live/Dead SYTO 9/propidium iodide bacterial viability kit (L1352) was obtained from Invitrogen. BSA (BAH64-0100) was obtained from Equitech-Bio. All reagents were stored according to the supplier's specifications and used as received. Millipore water (>18 MΩ-cm) was used in all experiments. All electrolyte solutions for electrochemical measurements were filtered using a 0.22-μm pore size Millex filter unit (Merck Millipore Ltd.).

Instrumentation. Electrochemical measurements were performed using a CHI model 920C potentiostat (CH Instruments) with the two-electrode cell placed in the grounded stage. Ag/AgCl in a saturated KCl solution was used as a reference and counter-electrode. For SECM approach curve measurements, a video microscope (CCD camera; Infinity2-1; Caltex lens; VZ-400; Caltex) was used.

Optical Imaging and Data Analysis. Samples were imaged during and after printing using bright-field illumination conditions on an inverted Zeiss Axiovert microscope with an ORCA-Flash 2.8 scientific-grade complementary metal oxide semiconductor camera (Hamamatsu) controlled by HCImage Live software (Hamamatsu). After the fabrication precursor was removed by melting and washing, bacterial growth within the microtraps was monitored using phase-contrast microscopy for 2–5 h at 37 °C on an inverted light microscope (Nikon TS100) housed inside an incubator (InVivo Scientific). The microtraps were then removed from the incubator and transported to the scanning electrochemical microscope for height, permeability, and pyocyanin measurements over time as the *Pseudomonas aeruginosa* populations continued to grow at room temperature.

Immediately after the final SECM measurement for pyocyanin, each sample was fixed chemically in 2.5% glutaraldehyde and stored at 4 °C. The fixed samples were then stained using a Live/Dead BacLight bacterial viability kit for 30 min before imaging using a Leica SP2 acousto-optic beam splitter confocal microscope equipped with a 40×, 1.25 N.A. oil-immersion objective. Confocal fluorescence images were acquired as a *z*-scan series (voxel height = 244 nm on the *z* axis) as described previously (1, 2). The number of cells in each microtrap was obtained from 3D volume reconstructions from confocal image stacks by either direct counting or finding the volume occupied by the cells by setting a threshold manually and then calculating the number of cells present by dividing that volume by the nominal volume of a *P. aeruginosa* cell (assuming that each cell is a cylinder measuring 1.5 μm in height and 0.75 μm in diameter). All image processing and analyses were done using ImageJ (National Institutes of Health) and/or FIJI (3).

Measurements of SECM Approach Curves or SECM Imaging. To obtain the SECM approach curves or SECM imaging using the prepared platinum ultramicroelectrode, the tilt of glass substrate was adjusted using two steps. First, using the leveler, the substrate tilt was coarsely adjusted. The coarsely adjusted tilt was finely controlled using the video microscope. Because the orientation of the focused ion beam (FIB) milling was adjusted perpendicularly to the body of the platinum ultramicroelectrode, we aligned the substrate perpendicular to the body of the platinum ultramicroelectrode on *x* and *y* axes using the video microscope with less than 0.1° offset. This procedure aligns the surface of the FIB-milled platinum ultramicroelectrode parallel to the substrate, thus enabling the closer approach. The FIB-milled platinum tips were prepared as reported elsewhere (4). Furthermore, to avoid electrostatic damage (ESD) on the electrode surface and thereby, maintain the inlaid shape of the platinum ultramicroelectrode, we followed the method of ESD protection reported by Nioradze et al. (5). With all of the ESD damage protection, the measurement of the SECM approach curve was carried out in a humidity-controlled room with higher than 30% relative humidity at 22 °C. All SECM measurements are described in greater detail elsewhere (6).

Characterization of the Microtrap Height and Permeability to FcMeOH Using SECM. The details regarding the experimental microtrap height and permeability measurements and the finite element simulations used to fit the data are described elsewhere (6).

Calibration Curve for Pyocyanin and the Quantification of Pyocyanin Produced from the Trapped *P. aeruginosa*. To construct the calibration curve for pyocyanin, an aliquot of a known concentration of pyocyanin solution was required. The commercially available pyocyanin is the oxidized form, which undergoes a two-electron transfer reaction in solution. However, the electrochemical reduction of oxidized pyocyanin at the platinum tip generates a polymerization side reaction during or after the electrochemical reaction, where the polymer is also redox-active (7, 8). Therefore, the platinum tip response and thus, the quantitative analysis can be hurt by the blocked electrochemical reaction as well as the larger capacitance caused by the polymer on the platinum surface. Such an effect is more serious when the tip size gets smaller than 5 μm in diameter, whereas a millimeter-sized electrode is influenced negligibly. To avoid the side reaction of polymerization by the direct electrochemical reduction of pyocyanin at the platinum tip, we electrochemically generated the reduced pyocyanin using a 5-mm-diameter platinum substrate electrode (Fig. S1*A*). When the platinum substrate electrode reduces the pyocyanin aliquot, a 5-μm-diameter platinum tip positioned 2 μm above the platinum substrate only senses the reduced pyocyanin as a bulk solution (Fig. S1*A*). In this unique SECM setup, called substrate generation/tip collection (SG/TC) mode, we could construct a calibration curve in the range of 2–120 μM pyocyanin, showing a good linear relationship between steady-state current of the platinum tip and the pyocyanin concentration (Fig. S1*B*). The SG/TC mode in this SECM setup allows for quantitative measurements to be made without fouling the tip and also, enhances the sensitivity of the measurements because of the closer distance between the platinum tip and the platinum substrate.

In the real microtrap chamber system, only the reduced form of pyocyanin is generated by bacteria within a microtrap and diffused out from the microtrap, whereas there is no pyocyanin in the external bulk solution. Thereby, the entire chamber serves as a generator of reduced pyocyanin-like platinum substrate in the SG/TC mode, whereas the platinum tip is collecting the reduced pyocyanin at 2 μm above the microtrap roof. To make sure that the calibration curve constructed from the SG/TC setup using platinum substrate–platinum tip could be applied to the platinum tip and microtrap chamber system, the current response vs. distance behavior from both systems were compared using

a finite element simulation (Fig. S2 *A* and *B*). The subdomain settings of the simulation with the microtrap chamber system are presented in Fig. S3. For this simulation, the roof permeability was set to the diffusion-limited case; thus, no diffusion barrier for pyocyanin was considered. Also, we set the uniform concentration of pyocyanin inside the microtrap, assuming that the pyocyanin production in the microtrap and its diffusion out from the microtrap are in equilibrium (i.e., steady state). Indeed, pyocyanin concentration monitored over the time showed a steady-state behavior after 6–10 h of growth at room temperature (Fig. S4). In addition, the planktonic bacteria in the microtrap can homogenize the pyocyanin concentration inside the chamber. In this regard, the assumption of the uniform concentration of pyocyanin within the microtrap at the steady state would be plausible in the simulation (Fig. S2*B*). Because the microtrap dimension is much larger than the diameter of the platinum tip, the platinum tip senses the reduced pyocyanin generated from the bacteria within the trap as the bulk. Both of the systems showed the nearly identical current vs. distance behavior, confirming that the constructed calibration curve can be used for the real measurement where the tip current is measured over the microtrap (Fig. S2*C*). For the real microtrap, the tip current is the function of roof permeability as a diffusion barrier of pyocyanin, where the tip current decreases as roof permeability gets smaller than the diffusion-limited case as shown in Fig. 2*C*. Thereby, the measured permeability of the roof is used as an attenuating factor to convert the measured tip current to the pyocyanin concentration using the calibration curve. For example, all of the currents were measured at 2 μm (i.e., 0.8 *d*/*r*) above the roof, where the current ratio between the roof permeability of 0.12 cm/s and the diffusion-limited case is 0.86 (Fig. 2*C*). Hence, the pyocyanin concentration is calculated as below:

$$[\text{pyocyanin}](\mu\text{M}) = \frac{\text{measured tip current (pA)}}{0.86 \times 0.409\ (\text{pA}/\mu\text{M})}.$$

Transfer Pathway of the Autoinducer Signal Produced by a *P. aeruginosa* Δ*phz* Aggregate to Neighboring Community. We simulated how the *P. aeruginosa* QS autoinducer signal molecule C_4-HSL generated by the signal-producer (Δ*phz*) cells diffuses from one chamber to another within the side-by-side 8-pL microtrap system using a finite element analysis. Despite the uncertainty that the signal molecule production rate reaches at steady state or steadily increases, it is obvious that the significantly high concentration of signal molecules is accumulated in the chamber; thus, it triggers the QS (i.e., pyocyanin production) and maintains its level at steady state, which is shown in Fig. S4. In addition, the planktonic movements of bacteria in the microtrap can homogenize the concentration of the signal molecule within the chamber. Based on these considerations, we assume the uniform concentration of signal molecules in the chamber of the signal-producer (Δ*phz*) cells in this time-dependent simulation. Fig. S5 displays the unsymmetrical concentration profile of the signal molecule at 30 min, which is generated from the right side of the microtrap, as the signal diffuses from the chamber into the bulk solution. The calculated signal flux through the 8-μm-thick shared wall between the two chambers is ∼50% higher than through the microtrap roof. For this simulation, the permeability measured by SECM experiments (6) was defined on the boundary of the chamber. Overall, the C_4-HSL signal molecules produced by the Δ*phz* aggregates are mainly transferred to the neighboring Δ*rhlI* community directly through the 8-μm separation distance, which was defined by the shared wall between the side-by-side microtrap chambers.

1. Connell JL, Ritschdorff ET, Whiteley M, Shear JB (2013) 3D printing of microscopic bacterial communities. *Proc Natl Acad Sci USA* 110(46):18380–18385.
2. Connell JL, et al. (2010) Probing prokaryotic social behaviors with bacterial "lobster traps." *MBio* 1(4):e00202–e00210.
3. Schindelin J, et al. (2012) Fiji: An open-source platform for biological-image analysis. *Nat Methods* 9(7):676–682.
4. Kim J, Izadyar A, Nioradze N, Amemiya S (2013) Nanoscale mechanism of molecular transport through the nuclear pore complex as studied by scanning electrochemical microscopy. *J Am Chem Soc* 135(6):2321–2329.
5. Nioradze N, et al. (2013) Origins of nanoscale damage to glass-sealed platinum electrodes with submicrometer and nanometer size. *Anal Chem* 85(13):6198–6202.
6. Kim J, Connell JL, Whiteley M, Bard AJ (2014) Development of a versatile *in vitro* platform for studying cellular interactions using micro-3D printing and scanning electrochemical microscopy. *Anal Chem*, in press.
7. Láng GG, Barbero CA (2012) *Laser Techniques for the Study of Electrode Processes* (Springer, Dordrecht, The Netherlands).
8. Sharp D, Gladstone P, Smith RB, Forsythe S, Davis J (2010) Approaching intelligent infection diagnostics: Carbon fibre sensor for electrochemical pyocyanin detection. *Bioelectrochemistry* 77(2):114–119.

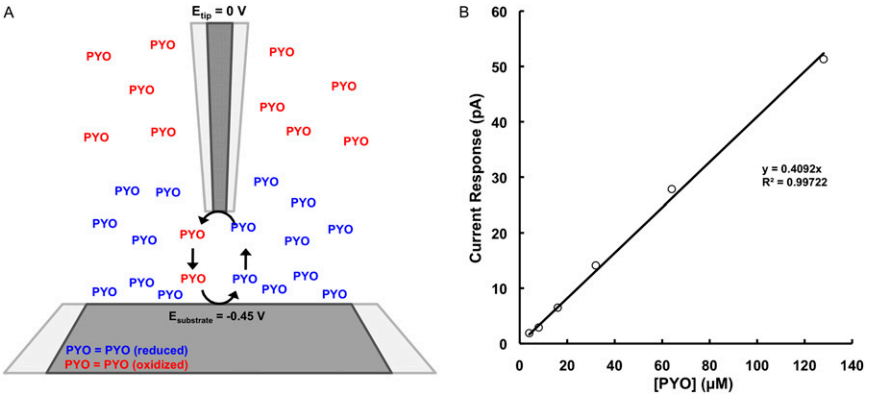

Fig. S1. (*A*) Schematic of the SG/TC setup for generating the reduced form of pyocyanin (blue) from a bulk solution of oxidized pyocyanin (red) using a large platinum substrate (5 mm in diameter) biased at −0.45 V vs. Ag/AgCl and the collection of the reduced pyocyanin (blue) by the platinum ultramicroelectrode tip at 0 V vs. Ag/AgCl. (*B*) The calibration curve for reduced pyocyanin constructed using the SG/TC setup shows that the current response at the platinum tip displays a linear correlation with the concentration of reduced pyocyanin in the range of 2–120 μM when the tip is held at a fixed distance of 2 μm above the large platinum substrate. PYO, pyocyanin.

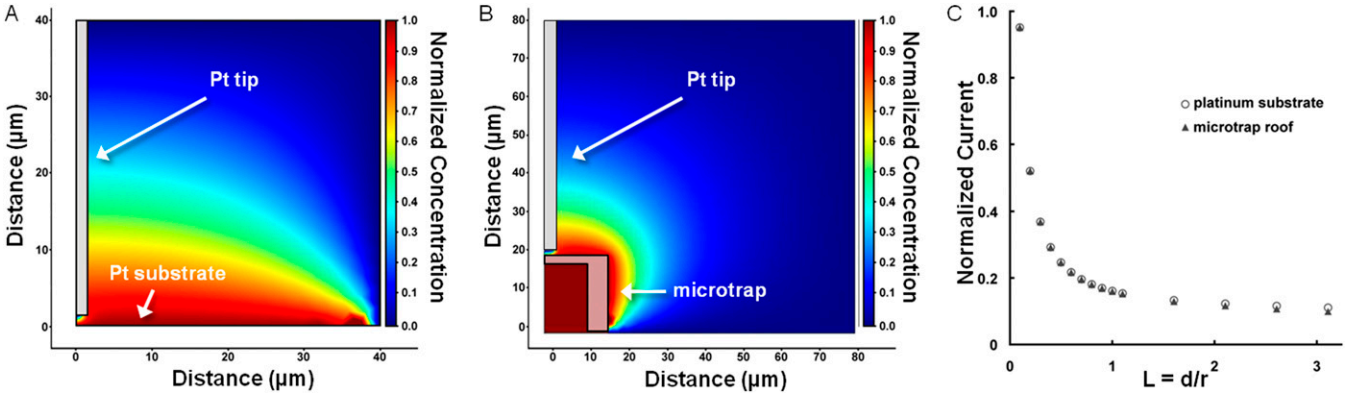

Fig. S2. (*A* and *B*) Two-dimensional axial symmetric cross-sections of the simulated concentration profile of the reduced pyocyanin (red) around (*A*) the platinum (Pt) tip–Pt substrate and (*B*) the Pt tip–microtrap systems. The Pt tip is held at 2 μm above each substrate. (*C*) The respective theoretical SECM approach curves for the simulations in *A* and *B* using $a = 2.5$ μm and a ratio of the glass sheath diameter to the electrode diameter (RG) = 1.4 of the Pt tip. The open circles and filled triangles correspond to the current response at the Pt tip over the Pt substrate and the microtrap, respectively.

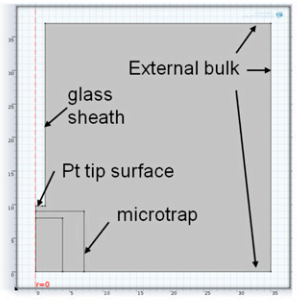

Sub-domain	Settings	
Outside microtrap	Initial value	$C_c = 0$
	electrode surface	Concentration ($C_{0,c}$), 0
	Glass sheath	No flux
	Outer roof and wall of microtrap	flux, $k_{c,c}$ =K, $C_{b,c}$= c2
	External bulk	Concentration ($C_{0,c}$), 0
Microtrap	Initial value	C_{c2}=1
	Inner roof, wall, and bottom of microtrap	Concentration ($C_{0,c2}$), 1
	Outer roof, and wall of microtrap	flux, $k_{c,c2}$ =K, $C_{b,c2}$= c2

Fig. S3. Subdomain settings for the finite element simulation of the Pt tip–microtrap system.

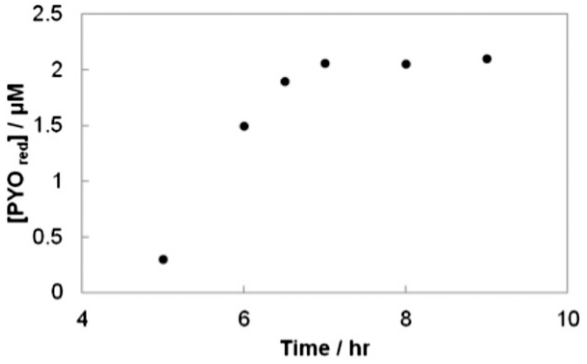

Fig. S4. The pyocyanin (PYO) concentration monitored above the microtrap over time.

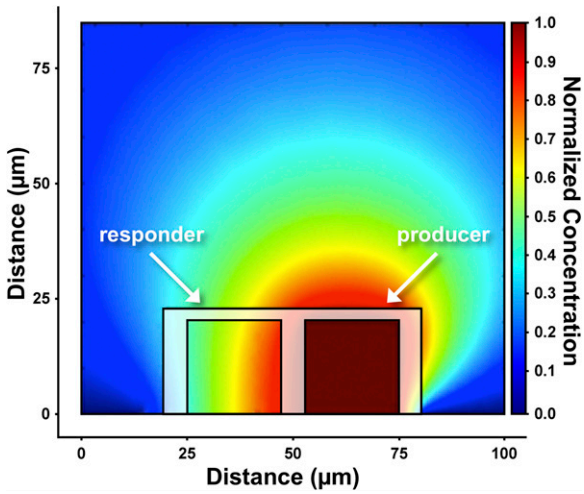

Fig. S5. 2D cross-section of the simulated concentration profile of the C_4-HSL signal molecule made by the *P. aeruginosa* Δ*phz* cells in (*Right*) the producer chamber of the side-by-side microtrap design shows that the most efficient diffusion pathway to transfer the signal between the neighboring chambers is directly through the 8-μm-thick shared wall. The simulation indicates that the signal flux from (*Right*) the producer chamber to (*Left*) the responder chamber is ∼50% higher through the 8-μm-thick wall than the diffusion rate through the microtrap roof.